Real-time Awake Animal Motion Tracking System for SPECT Imaging

J. S. Goddard, *Member, IEEE*, J. S. Baba, *Member, IEEE*, S. J. Lee, A. G. Weisenberger, A. Stolin, J. McKisson, and M. F. Smith, *Member, IEEE*

***Abstract*– Enhancements have been made in the development of a real-time optical pose measurement and tracking system that provides 3D position and orientation data for a single photon emission computed tomography (SPECT) imaging system for awake, unanesthetized, unrestrained small animals. Three optical cameras with infrared (IR) illumination view the head movements of an animal enclosed in a transparent burrow. Markers placed on the head provide landmark points for image segmentation. Strobed IR LED's are synchronized to the cameras and illuminate the markers to prevent motion blur for each set of images. The system using the three cameras automatically segments the markers, detects missing data, rejects false reflections, performs trinocular marker correspondence, and calculates the 3D pose of the animal's head. Improvements have been made in methods for segmentation, tracking, and 3D calculation to give higher speed and more accurate measurements during a scan. The optical hardware has been installed within a Siemens MicroCAT II small animal scanner at Johns Hopkins without requiring functional changes to the scanner operation. The system has undergone testing using both phantoms and live mice and has been characterized in terms of speed, accuracy, robustness, and reliability. Experimental data showing these motion tracking results are given.**

I. Introduction

Oak Ridge National Laboratory (ORNL), Thomas Jefferson National Accelerator Facility (Jefferson Lab), and the University of Maryland are collaborating in the development of an advanced high-resolution SPECT instrument to image awake, unanesthetized small animals. Previous work has been described here [1]-[4]. Animal brain studies are prime examples where anesthetic agents or physical restraints are of greatest concern in affecting the results. This technology allows functional imaging studies to be performed on animals without the use of anesthetic agents and has further clinical applications on human patients that cannot remain still (Parkinson's patients, small children, etc.) during a PET or SPECT scan.

A key component of this new device is the real-time optical pose measurement and motion tracking system that provides 3D position and orientation during the single photon emission computed tomography (SPECT) imaging scan. The tracking apparatus is an integral part of the scanner and is designed to measure the spatial position and orientation of the animal at a rate of at least 15 frames per second with sub-millimeter accuracy. The pose data is time stamped along with SPECT list mode data to enable correction of motion blur after the scan during image reconstruction.

Further developments have been made to the tracking system. An improved three camera design provides a small physical package that is fully integrated within a Siemens MicroCAT II scanner without interfering with the scanner functionality. This enhanced system is faster, more accurate, and more robust than previously reported results. The system and scanner are presently undergoing testing at John Hopkins University.

II. Tracking System Description

The tracking system uses optical infrared imaging to view an animal enclosed in a transparent burrow located between the SPECT detector heads developed by Jefferson Lab. Three cameras along with concentric IR ring lights illuminate retro-reflective markers placed on the animal's head. The lights are synchronized and pulsed in stages to freeze motion while minimizing reflections. The three camera image acquisition system acquires images of the awake animal through a wide range of motion with improved accuracy over the binocular stereo used previously. Any loss of tracking during a scan is significantly reduced through the camera redundancy where a 3D measurement can be calculated when a marker is visible from only two of three cameras.

Figs. 1 and 2 below show the scanner and SPECT detectors along with the tracking cameras and mouse burrow. The three cameras are mounted in a triangular pattern in the rear of the scanner facing the front of the transparent tubular burrow containing the animal. The cameras are raised above the center of the burrow and angled to look down on top of the head of the animal. An LED ring light is mounted around each camera's lens to near coaxially illuminate the retro-reflective markers placed on the animal's head. The markers are spherical with one side flattened for attaching to the body. Pulsing of the lights is synchronized with the image frame acquisition from the cameras. Slight staggering of the pulse timing, however, removes adjacent ring light reflections. This

Manuscript received November 15, 2008. This paper was prepared by the Oak Ridge National Laboratory, Oak Ridge, Tennessee, 37831-6285, operated by UT-Battelle, LLC for the U.S. Department of Energy under contract DE-AC05-00OR22725.

J. S. Goddard, J. S. Baba, S. J. Lee are with Oak Ridge National Laboratory, Oak Ridge, TN 37831 USA (telephone: 865-574-9034, e-mail: goddardjsjr @ornl.gov).

A.G. Weisenberger, A. Stolin, J. McKisson are with Jefferson Lab, Newport News, VA, USA, (telephone: 757-269-7090, e-mail: drew @jlab.org).

M. F. Smith. is with University of Maryland, Baltimore, MD 21201 USA (e-mail: msmith7@umm.edu).

Authorized licensed use limited to: Oak Ridge National Laboratory. Downloaded on March 23,2010 at 15:23:08 EDT from IEEE Xplore. Restrictions apply.

is accomplished by sequentially pulsing the ring lights with submillisecond timing separation so that each camera is exposed only during its ring light activation. The result is that only the reflection from the one light due to the holder is visible in each image.

Software on the tracking PC consists of a graphical user interface and a functional code base that performs image acquisition, automatic marker segmentation, reflection rejection, marker correspondence, tracking, and 3D pose calculation. The motion tracking system is also time stamped as is the detector system so that list mode SPECT detector data can be motion compensated as part of reconstruction after the scan is complete.

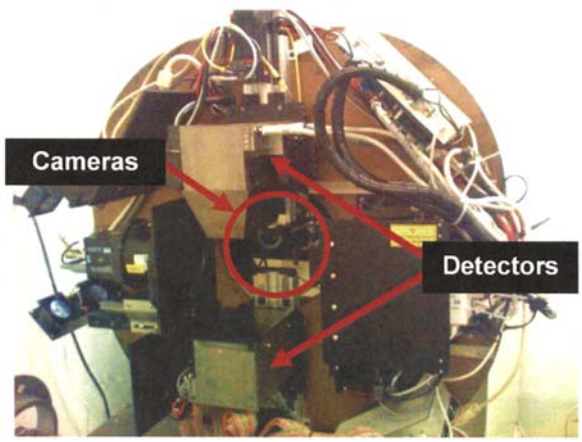

Fig. 1. Front view of scanner showing tracking system hardware and location with respect to SPECT detectors. Optical hardware is facing towards the front of the scanner.

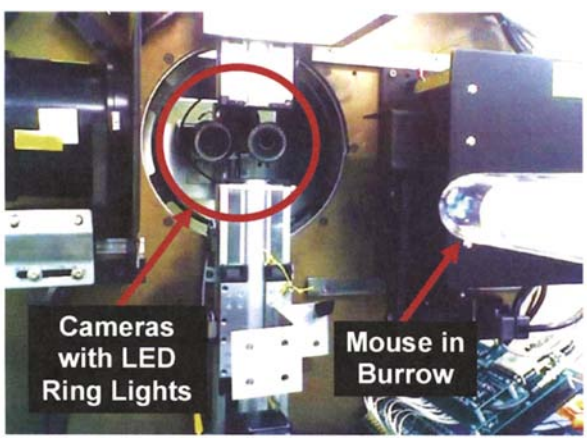

Fig. 2. Picture of mouse burrow and relationship to optical hardware mounted at rear of scanner

III. Measurement Progress

The overall measurement approach is shown in Fig. 3. Simultaneous images from the three calibrated cameras are first segmented to determine marker positions. Correspondence of markers between images is performed next with filtering to remove invalid reflections. 3D positions are then calculated, tracked, and fit to an initial model. The initial model is formed from the first valid measurement position of the markers after tracking begins.

Position and orientation are determined relative to the model. A minimum of three marker points is required for 3D measurement although more can be used for redundancy. A topographic model is defined that permits the determination of point correspondence for cases where a point is obstructed or where an extraneous point is present. An initial offline camera calibration is performed to determine both intrinsic (focal length, camera center, and distortion) and extrinsic calibration parameters for each camera that includes the relative coordinate transformations among the three cameras.

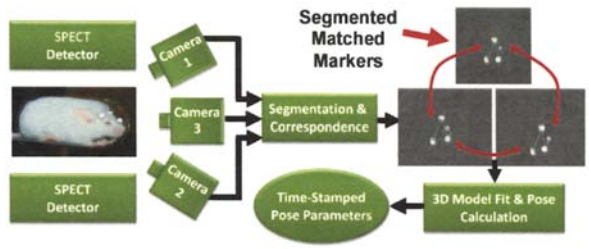

Fig. 3. System functional block diagram for motion tracking showing measurement steps for calculating 3D position and orientation

Significant progress has been made from earlier results [2], [4]. The principal improvements have been in camera calibration, segmentation, correspondence, false marker rejection, and 3D calculation. A full three-camera optimization of the camera calibration parameters has been newly developed to improve accuracy of the parameter estimates and to ensure consistent measurements among all cameras. Segmentation has been improved in speed and reliability through the use of an adaptive hysteresis thresholding technique. Tracking speed and reliability have been improved through a region of interest method. Tracking is also improved using estimates from previous measurements. Better accuracy for 3D calculations is obtained from least-squares error fitting of optimized centroids with respect to the nearest epipolar line.

A. Calibration

Intrinsic offline calibration for camera parameters and SPECT detector calibration have been previously described [2]. A full extrinsic parameter optimization has been developed for the three-camera setup that simultaneously optimizes all three camera parameters. In earlier work only pairs of cameras were optimized giving slightly inconsistent results between pairs. This optimization minimizes the sum of the squared error between the measured and projected image points. The camera to camera transformations, $\mathbf{T}_{12}$ and $\mathbf{T}_{13}$ are determined, where $\mathbf{T}_{xy}$ is the homogeneous transformation matrix from camera x to camera y while the intrinsic

Authorized licensed use limited to: Oak Ridge National Laboratory. Downloaded on March 23,2010 at 15:23:08 EDT from IEEE Xplore. Restrictions apply.

parameter values are further optimized. This overall result provides the minimum error for three camera 3D calculations and provides consistency for calculation using sets of two cameras.

B. Segmentation and Correspondence

Marker segmentation has been improved through the use of an adaptive hysteresis thresholding method to extract marker locations in the image. Markers are characterized by regions of varying brightness with a central core of high brightness. The central region is expanded using this method to cover the entire marker without needing a time-consuming region growing technique. After segmentation, the markers are filtered to eliminate non-marker regions and the centroid is calculated.

Point correspondence has been made more accurate and robust through inclusion of stereo correspondence constraints including ordering, uniqueness, and continuity [8][9]. Points on the same epipolar line for pairs of cameras or that meet the trifocal tensor relation for the camera triplet are candidates for matches. The above constraints are applied to these points to determine the correct correspondences.

Points meeting these criteria are uniquely determined. In many cases, matches will not be found for all points due to obstructions or mouse movement out of the camera view. Measurements can be made where marker point correspondences are present in any two of the three camera views.

C. Pose Measurement

At least three marker points are required for a pose measurement. The segmentation and correspondence operations described above provide marker centroid measurements from one or more pairs of cameras for each marker point. Using an optimal triangulation method from Hartley [5], the marker centroids from camera pairs are corrected to minimize the geometric error subject to the epipolar constraint as given in [2]. For each set of matched point measurements, a least square inhomogeneous method is applied to calculate the 3D coordinates with respect to the base reference coordinate frame of the reference camera. These points are matched to an automatically defined model so that both 3D position and orientation may be calculated [7]. The difference in orientation and translation between the current position and initial position defines the relative head motion over the scan. A region of interest within the image is used to track the head based on prior measurements to improve speed and ignore motion outside the head region.

IV. Results

Experimental results have been obtained with the SPECT system using the three-camera system to track phantoms, live mice, and live mice scans. Full six degree of freedom motion compensated reconstruction has been achieved using the live tracking data. Initial phantom testing and live mouse testing have been performed on the scanner at Johns Hopkins with SPECT scans ranging from 20 to 30 minutes in length. A static test using a stationary phantom during a full 360 degree gantry rotation shows the baseline noise levels in Fig. 4. These plots show the pose measurements over time as given by the sample index. These results also show some residual motion in the gantry over the scan. Generally translation noise standard deviation is 0.1 mm or less and orientation noise standard deviation is 0.2 degrees or less. See [4] for more detailed noise measurements. A live mouse scan is similarly shown in Fig. 5 over a 30 minute run. Missed measurements during the scan have been removed from these plots. This motion pattern is typical for a live mouse in that quick impulsive movements are interspersed with slower more gradual changes in position. Loss of measurements during a scan has been reduced over that reported previously [4]. Valid measurement rates over multiple live mouse runs were 94% or greater compared to 78% in previous results.

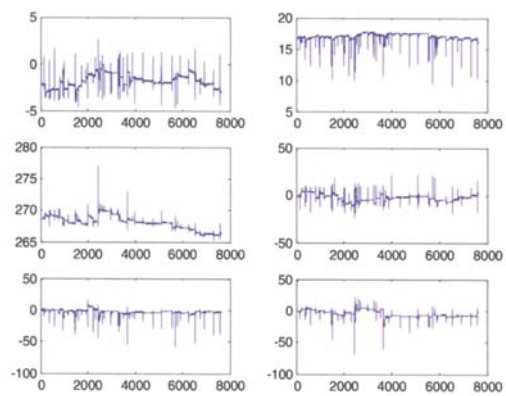

Fig. 4. Static test pose measurement results on stationary phantom with rotating gantry. Variables shown in the plots are x, y, z translation, and yaw, pitch, roll orientation from left to right and top to bottom. Translation units are in mm while orientation angles are in degrees. Horizontal axis is the sample index proportional to time.

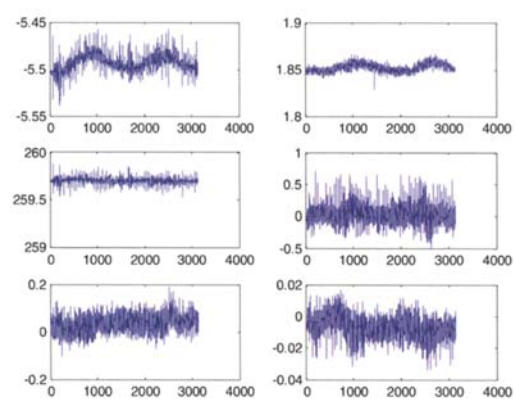

Fig. 5. Live mouse pose measurement results over 30 minute SPECT scan. Units and axes are the same as Fig. 4.

Authorized licensed use limited to: Oak Ridge National Laboratory. Downloaded on March 23,2010 at 15:23:08 EDT from IEEE Xplore. Restrictions apply.

Fig. 6 below shows a composite slice 3D reconstruction from a SPECT scan. Shown are the uncompensated, motion compensated, and static views. For reference, a CT scan of the same mouse gives the corresponding anatomical regions. The compensated image is seen to have a significant improvement in image quality over the uncompensated data with motion blur reduced considerably. Additional information on the SPECT system is given by Weisenberger, et al. [10]. For details on the motion compensated reconstruction, see Stolin, et al. [11].

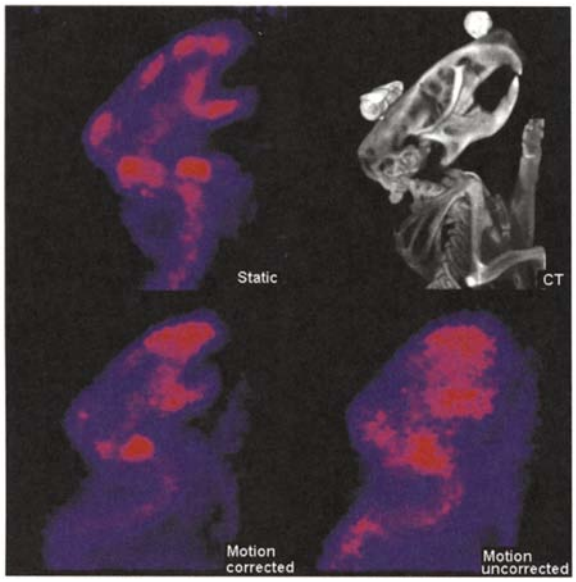

Fig. 6. Live mouse 3D SPECT reconstruction results are shown above that demonstrate the improvement in image quality with motion compensation using the tracking measurements over uncompensated 3D reconstruction. A slice of the 3D results shows uncorrected, corrected, and a static scan of the same mouse for comparison. Also shown is the corresponding CT slice giving anatomical features.

V. Conclusions

Improvements in the real-time motion tracking system for an awake animal SPECT scanner have been described. This system is fully integrated within a commercial scanner and has been demonstrated to reliably and accurately measure head position and orientation of a mouse through SPECT scans of more than 30 minutes. The improvements include better segmentation of marker points, better correspondence between images, and more accurate 3D calculations. The motion tracking measurements have been validated through the improvements in image quality obtained through the 3D reconstruction with motion correction. Plans are to continue studies with live mice concentrating on further improving reliability and accuracy for motion tracking.

Acknowledgment

Support for this research came from the DOE Office of Biological and Environmental Research, the DOE Office of Nuclear Physics, and National Institutes of Health grant U24 CA92871.

References

[1] A. G. Weisenberger, B. Kross, S. Majewski, V. Popov, M. F. Smith, V. H. Tran, B. Welch J. Baba, J. Goddard, M. Pomper, and B. Tsui, "Instrumentation Development of a SPECT-CT System to Image Awake Mice," Proc. IEEE Medical Imaging Conference, San Diego, November 2006.

[2] S. S. Gleason, J. S. Goddard, M. J. Paulus, J. S. Baba, S. Majewski, M. Smith, T. Tran, A. Weisenberger, B. Welch, R. Wojcik "Real-time, high-accuracy 3D tracking of small animals for motion-corrected SPECT imaging," Proc. IEEE Nuclear Science Symposium and Medical Imaging Conference, Rome, Italy, October, 2004.

[3] A. G. Weisenberger, B. Kross, S. Majewski, V. Popov, M. F. Smith, B. Welch R. Wojcik, S. Gleason, J. Goddard, M. Paulus, and S. R. Meikle, "Development and Testing of a Restraint Free Small Animal SPECT Imaging System with Infrared Based Motion Tracking," Proc. IEEE Medical Imaging Conference, Portland, November 2003.

[4] J. S. Goddard, J. S. Baba, A.G. Weisenberger, and M. F. Smith, "Improved Pose Measurement and Tracking System for Motion Correction of Awake, Unrestrained Small Animal SPECT Imaging," *Conference Record, IEEE NSS/MIC*, Honolulu, 2007.

[5] R. Hartley and A. Zisserman, *Multiple View Geometry in Computer Vision*, Cambridge: Cambridge University Press, 2000.

[6] A. G. Weisenberger, J. S. Baba, B. Kross, S. Gleason, J. S. Goddard, S. Majewski, S. R. Meikle, M. Paulus, M. Pomper, V. Popov, M. F. Smith, B. Welch, and R. Wojcik,, "Dual Low Profile Detector Heads for a Restraint Free Small Animal SPECT Imaging System," Proc. IEEE Nuclear Science Symposium and Medical Imaging Conference, Rome, Italy, October 2004.

[7] B. Horn, "Closed-form solution of absolute orientation using unit quaternions," Journal of the Optical Society of America, 4, pp. 629-642, April 1987.

[8] O. Faugeras and Q-T. Luong, *The Geometry of Multiple Images*, Cambridge: The MIT Press, 2001.

[9] H. H. Baker and T. O. Binford. "Depth from edge and intensity based stereo," Proceedings 7th Int. Joint Conf. on Artificial Intelligence, pp 631--636, Vancouver, BC, Canada, August 1981.

[10] A.G. Weisenberger, J.S. Baba, J.S. Goddard, B. Kross, S.J. Lee, S. Majewski, J. McKisson, M. Pomper, V. Popov, J. Proffitt, M.F. Smith, A. Stolin, and B. Tsui, "Awake Animal SPECT: Overview and Initial Results," *Conference Record, IEEE* NSS/*MIC*, Dresden, 2008.

[11] A.V. Stolin, J. McKisson, A.G. Weisenberger, J.S. Baba, J.S. Goddard, S.J. Lee, and M.F. Smith, "Image Reconstruction for Awake Animal SPECT Imaging," *Conference Record, IEEE* NSS/*MIC*, Dresden, 2008.

Authorized licensed use limited to: Oak Ridge National Laboratory. Downloaded on March 23,2010 at 15:23:08 EDT from IEEE Xplore. Restrictions apply.